E. J. Engineering Sciences and Technology, Vol. 2:(2017),19-30
http://www.cessciencegroup.com

Punching Shear Behavior of Small SFRC Flat Plate

Farid H. ARNA'OT [1*], Ahmmad A. ABBASS [1], Ahmed A. ABU ALTEMEN [2], & Mustafa ÖZAKÇA [1]

[1] *Department of Civil Engineering, Gaziantep University, TURKEY.*
[2] *Department of Division of Engineering Affairs, University of Mustansiriya, IRAQ*
Correspondence email: farnaot@gmail.com

Received 15 February 2017; Accepted 21 July 2017

ABSTRACT

Resistance of steel fiber reinforced slabs to punching is extensively investigated, which showed that the steel fibers enhanced the ultimate slab resistance made of normal strength concrete. Current work involved the testing of three small high strength concrete slabs. The slabs were of 500 mm square sides, and of 60 mm thickness. The slabs were reinforced by two steel fiber dosages 0.75 % and 1.25 %, in addition to conventional reinforcement bars of moderate ratio. The results showed that the steel fibers have slightly effect on the ultimate strength of high strength concrete slab compared to that obtained for normal strength concrete. The results were used in comparison between ACI318 and EC2 provision related to punching shear of normal concrete slabs, moreover, three proposed models found in literature were employed in comparisons. It is concluded that the current codes provision are significantly underestimating the punching shear strength for high strength concrete slabs.

Keywords: flat plate-column connection, punching shear, reinforced concrete, small slabs, steel fiber.

1. Introduction

Slab hold by column without beams, drop panels, and capital, are highly involved in building that had critical space, and such thing is required in car parking and tunnels. This type of structure is often governed by two-way shear failure and often occurs suddenly and catastrophically, therefore this type of failure should be carefully investigated and avoided. In general, the shear forces are resisted by the concrete in terms of concrete strength and by the conventional flexural and shear reinforcement with different level of activity. One of the most active ways to improve the behavior of the slab strength is using fibers. Many types of fibers had long been employed in order to enhance the mechanical properties of concrete, mostly to control the propagation of cracks. It showed that the fibers are active in transferring the stresses through the cracks (Gouveia, et al., 2014; Choi, et al. 2007), it also showed that the activity of the fibers is after initiation of the cracks (Shah 1981). Punching shear resistance of slab made from Steel Fiber Reinforced Concrete (SFRC) is extensively studied (Gouveia, et al., 2014; Abadel, et al., 2014; De Hanai & Holanda, 2008; Harajli, et al., 1995; Shaaban & Gesund, 1994; Swamy & Ali, 1982) for all; the steel fiber has significantly enhancing the ultimate punching shear strength, energy absorption, and ductility.

Many models were applied in order to predict the steel fiber reinforced concrete (SFRC) punching shear ultimate load; because there are no available codes provisions on such structure with steel fiber reinforcement concrete. Most of the proposed models are employing the codes equation related to punching shear of flat plate made with plain concrete.

Current work presents an experimental work on three small slabs loaded by monotonic increasing load through a column stub located at the center of the slabs. The slabs were reinforced by steel fiber in addition to the conventional reinforcing bars. The tested slabs were made from high strength concrete, and high fine aggregate content compared to the total aggregate content, in order to increase the activity of the steel fiber in bridging the cracks, moreover the high fine aggregate content applied an early high strength.

2. Material and Methods

2.1 Slab Geometry and Materials

To check the slab resistance, three isolated flat plate of small size have been carried out; all specimens are of the same size of square concrete plates (500 mm × 500 mm × 60mm), same flexural reinforcement ratio (no special shear reinforcement) were used, but with different steel fiber dosages. Deformed bars of 5.3 mm diameter were used with ultimate and yield strength of 477 MPa and 400 MPa respectively, orthogonally placed at tension face as a single reinforcement layer with clear cover of 15 mm. and equally spaced in each horizontal directions $S_x = S_y = 52$ mm center-to-center (with reinforcement ratio equal to

1.1%) . All bars were bended with 90°, all free bends were tied to gather by additional one bar in each layer in compression face, as shown in Figure 1.

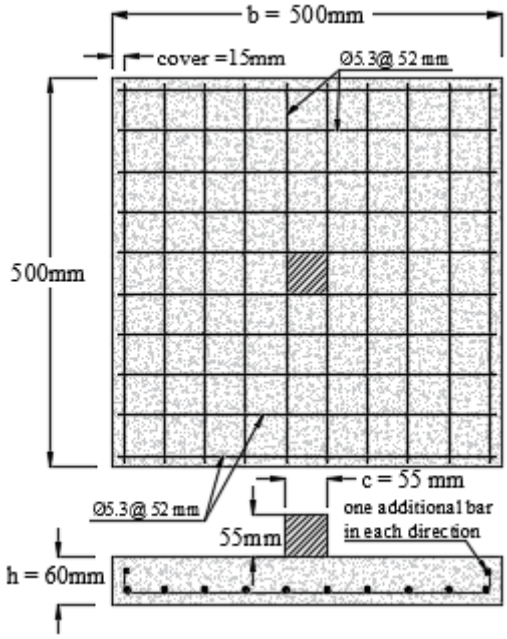

Figure 1. Slab geometry and reinforcement details.

The slabs were designed to reach 28-day standard cylinder (100 mm × 200 mm) compressive strength (f'_c) of 60MPa. The concrete mix included: 37 % of total aggregate were crushed stone coarse aggregate with maximum size of aggregate of 10 mm, 63 % of total aggregate were river sand, and Portland cement of type CEM II/ A-LL 42.5 R. 7.5 % of cement mass were replaced by silica fume. Moderate water percentage (W / cementitous materials = 0.43) was used. The moderate water percentage, high percentage of fine and cementitous materials that used, led to low slumps, therefore, 6.6 kg /m^3 of super-plasticizer were used, and Table 1 shows the percentage of mixed materials.

Table 1. Concrete mix.

Mix code	C kg/m^3	S.fm kg/m^3	S kg/m^3	G kg/m^3	W kg/m^3	SP kg/m^3	W/C
S0	465	35	1170	680	216	6.6	0.43

C; cement, S.fm; silica fume, S; river sand, G; crashing stone, W; water, SP; super-plasticizer

The concrete used in slabs was produced in three batches. For each batch, the aggregate was mixed together for 10 minutes, and five extra minutes for mixing with cement, silica fume and water. The super-plasticizer was added gradually before adding the steel fibers. During the manually addition of steel fiber, the mixer was rotated in its full speed

capacity, and then more 45 revolutions were rotated after completion the specified steel fiber amount in slow rotating rate. Two percentages of steel fiber (0.75 %, and 1.25 %) by weight of concrete were used, the SFRC slabs were compared to control slab of plain concrete (no steel fiber were used), and the employed steel fiber properties used are shown in Table 2.

Table 2. Steel fibers characteristic.

Type	Geometry	Density kg/m^3	l_f mm	D_f mm	l_f/D_f	Tensile strength MPa
KMX 55/30 BG	Hooked-ends	7850	30	0.55	55	1500

The experimental program included testing the mechanical properties of the concrete. In order to overcome the probable errors, the average of three standard cylinders was considered. Externally vibration was applied to SFRC, and internally rodding is applied to the plain concrete specimens.

2.2 Test Configuration

The cured two-way small-slabs and standard cylinders were tested under monotonic increasing load at the same testing day. The tested slabs were supported on special made support that included 8 points load, these points load are of steel half balls, which are distributed uniformly in central angle of 22.5 deg. and 200 mm radii as shown in Figure 2. The support and the steel half balls were designed to sustain the applied load so as not to deform and penetrate the concrete slabs due to stress singularity. The load applied through a steel plate of 55 mm sides in displacement rate of 0.4 mm/min. Two linear variable differential transformers gages (LVDTs) were placed beneath the center of slabs and 110 mm from the center in order to monitor the deflection of the slabs under loading.

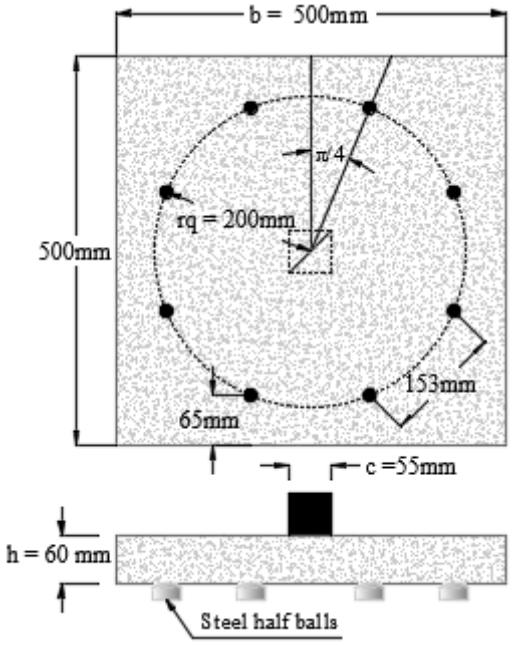

(a) (b)

Figure 2. (a) Test setup and (b) Supporting details.

3.Results and Discussion

3.1.Materials Properties

Table 3 shows the experimental results of the standard cylinders that are employed to obtain the compressive strength (f'_c) according to ASTM C39, the splitting tensile strength (f_{sp}) according to ASTM C496, and static Young's modulus according to ASTM C469. It is showed that, the steel fiber has a significant effect on the mechanical properties, where 1.25% of steel fiber enhanced the compressive strength by 11 %, however there was no improving to the tensile and the modulus of elasticity.

Many codes of practice have been adopted the square root of the compressive strength (such as ACI 318), which is good representing the punching shear strength, for specimens of reinforcement ratio $\rho > 0.5$, therefore, $\sqrt{f'_c}$ is used here to assess the strength of specimens in current work. Moreover, $\sqrt{f'_c}$ is relating to splitting tensile strength form of $f_{sp} = k\sqrt{f'_c}$, where k is a constant. Many values were proposed for the k for SFRC based on linear regression including the effect of steel fiber dosage (De Hanai & Holanda, 2008, Harajli, et al., 1995; Shaaban & Gesund, 1994). Adopting the two proposed equations by (De Hanai &

Holanda, 2008) and (Shaaban & Gesund, 1994), it is showed that a modification should be considered to represent the relation in current experimental results, where f_{sp} is related to $\sqrt{f'_c}$ according to Equation 1.

$$f_{sp} = \sqrt{f'_c} \times \left[\frac{196.25\, V_f}{w_c} + 0.95\right] \quad (1)$$

Where V_f is the steel fiber volume fraction, and w_c is the unit weight of the plain concrete.

Table 3. Concrete mechanical properties.

Spec. No.	Steel fiber V_f (%)	Age at day of test	f'_c (MPa)	f_{sp} (MPa)	E_c (GPa)
S0	0	34	53	7.1	38.13
S0.75	0.75	37	51	6.8	37.27
S1.25	1.25	37	59	7.0	37.41

3.2.Ultimate Slab Strength

Table 4 summarized the ultimate slab resistance, the central deflection, and the failures mode, It is shows that the inclusion of the steel fibers in concrete significantly enhanced the ultimate slab strength of specimen with 1.25% (by about 17%), however using 0.75 % of steel fiber, did not affect the behavior of slab. This is confirmed by the cylinder test as mentioned before. The tested results were compared with some data found in literature (Abadel, et al., 2014; De Hanai & Holanda, 2008; Harajli et al., 1995). For small SFRC slabs, details of specimens are shown in Table 4. The normalized ultimate strength was drawn in term of the steel fiber volume fraction as shown in Figure 3. The comparison showed that for all used data, the normalized ultimate slab strength is enhanced with increasing the steel fiber dosage in same rate. This can be represented by a linear expression such as in Equation 2,

$$\frac{P_u}{\sqrt{f'_c} b_o d} = (A \times V_f) + C \quad (2)$$

Where, A is the rate of normalized strength equal to 6.5 and C is the constant, which is significantly differed, due to many parameters. Two differences shows to have significantly effects, the type of specimens support, and the weak bond between the matrix and the reinforcement bars, where the bars in specimens investigated by the two references was not bended.

Table 4. Experimental characteristics of flat plate.

Spec.	P_u (kN)	δ_1[(a)] (mm)	Failure[(b)] type	Punching shape	$r_{0,\,test}$[(c)] (mm)	Angle of failure (deg.)
E0	79.63	3.9	P	Circle	218	17-22
E0.75	78.80	3.7	P	Circle	188	18
E1.25	93.28	4.0	P	Circle	179	18

[a] δ_1 are the displacement at the center that corresponding to ultimate loads P_u.
[b] P Refers to punching shear failure and, F refers to flexural failure.
[c] Radius of the critical punching crack taken as the longest size in ellipse and square.

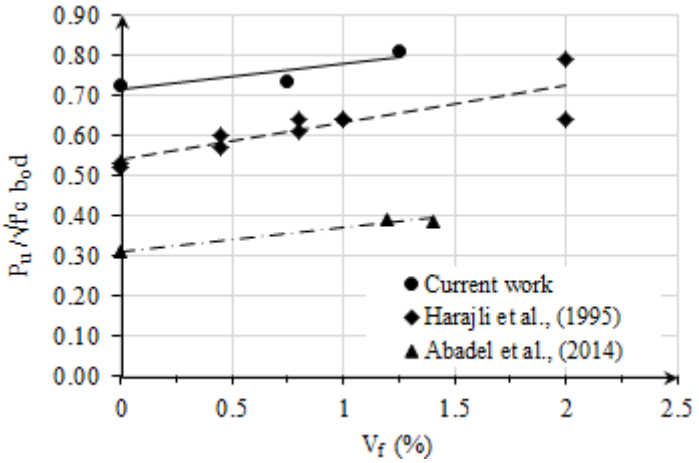

Figure 3. Comparison of the normlised ultimate strngth with data collected from litrature.

3.3.Load-Deflection Behavior

Figure 4a shows the displacement of the slabs at corresponding ultimate load, the figure includes the measured displacement for the two LVDTs used, where δ_1 refers to the displacement obtained from LVDT that placed at the center of the slabs, whereas the δ_2 is distanced 110 mm from the center. δ_1 is the highest value compared to δ_2 that showed less gradual displacement, which means that the cracks distanced more than 2d (where d is the effective depth) from the column face. Figure 4b shows the development of the displacements of δ_1 and δ_2 under the monotonic increased loading. The post displacements were hidden in this paper for further investigation. In general, the applied loads were continued until 40 % of its peak load. The first cracks were monitored via mini-camera placed beneath the slabs and connected to a computer. All curves are almost linear at the elastic stage (before first cracking), where the cracks initiated at low load 11 kN, 12 kN, and 18 kN for tested slabs of

0 %, 0.75%, and 1.25%, respectively, which are 14%, 15%, and 19% of the peaks load. The obtained first crack loads were within the percentage that obtained by (Swamy & Ali, 1982). After cracking, the slab E0 showed lowest deformation rate, whereas E1.25 was deflected with higher deformation rate, i.e., the load induced one unit deflection more than that required for E0, which means that adding steel fiber leads to reducing the deformation. It is worthless that all specimens exhibited short horizontal plateaus before reaching the deflection correspond to ultimate load.

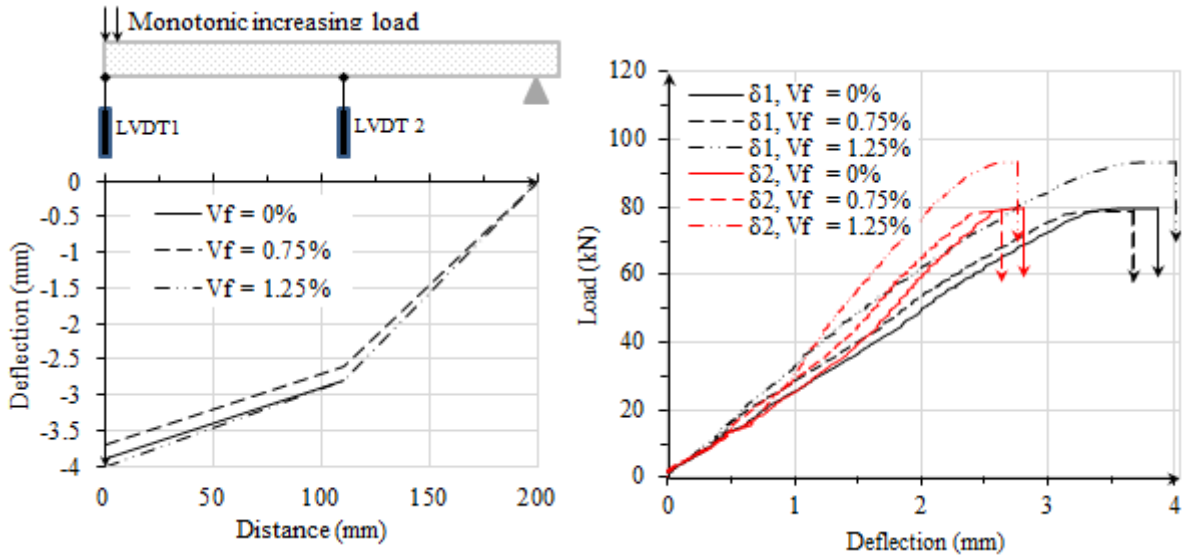

(a) (b)

Figure 4. (a) typical deflections along the slab width (b) Load-deflection at center and at distance 110 mm from the center

3.4.Failure Mode

The failed slabs were replaced from the test machine. The observed details, such as the actual critical shear crack perimeters were measured, types of failure were classified visually as listed in Table 4. In general, all specimens were failed due to pure punching shear effect, with different punching shapes. E0 (specimen without steel fiber) was failed with three types of crack patterns. The first is flexural horizontal cracks, which includes four cracks alignments with the edges of fictitious projection of column stub at the tension face; the second is a circle shape around the projection of the column stub and distance d from it. The main failure crack is of ellipse shape that exhibited extensive spalling, wide parts were fall that prevented the radial cracks from reaching the edges of slab, the major axis (218 mm ≈ 4.8d) of ellipse were exceeded the support points radii (r_q= 200 mm), Figure 5 shows the crack mode of the tested slab.

The failure shape of the specimen with 0.75 % steel fiber was the same as the E0 but with main failure crack of almost incomplete circle with radius equal to 2.3d from the column face. Significantly, different behaviors were shown in E1.25, where the flexural horizontal cracks did not show it up. The diameter of main punching crack was less than the other (4d from the face of column), with hair crack located within the main cracks area.

For all slabs, the inclination of cracks with the horizontal axis were 17°-22°, which is agreed with the finding of (Shaaban & Gesund, 1994; Gardner, 1990). It is concluded that the inclusion of steel fiber has slightly effect on failure shape, which is agreed with the conclusion of (Shaaban & Gesund, 1994).

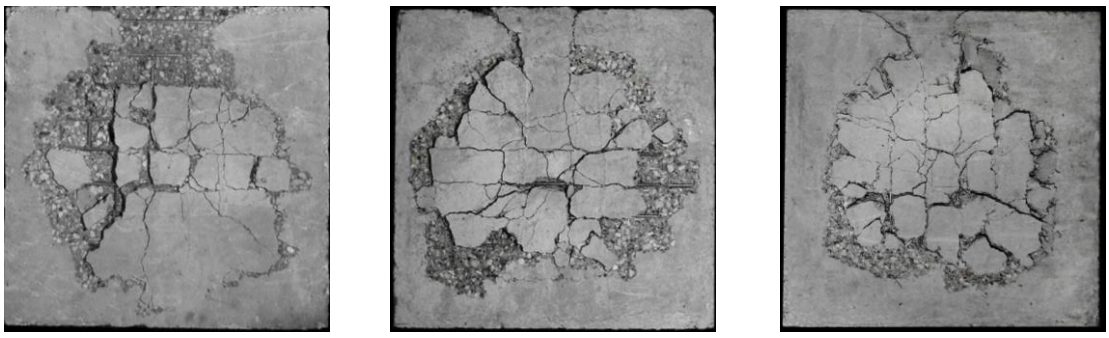

E0, Normal Concrete E0.75, SFRC, Vf = 0.75% E1.25, SFRC, Vf = 1.25%

Figure 5. Failure pattern of slabs.

Comparison of Experimental Ultimate Strength with Proposed Models

According to ACI318 and EC2

ACI318-14 adopted a minimum stress obtained from Equation 3 to predict the punching shear stress for normal concrete weight, where this stress is act on perimeter distances d/2 from the column face. This equation was derived from semi-empirical analysis method based on experimental results and the analysis basis on Column yield criterion.

$$\nu_c = 0.33\sqrt{f'_c} \tag{3a}$$

$$\nu_c = 0.17\left(1 + \frac{2}{\beta}\right)\sqrt{f'_c} \tag{3b}$$

$$\nu_c = 0.083\left(2 + \frac{\alpha_s d}{b_o}\right)\sqrt{f'_c} \tag{3c}$$

Where f'_c is the concrete compressive strength, b_o is the perimeter of critical shear crack, d is the effective depth, β is a ratio of long to short side of column, α_s equal to 40 for interior

column . It is shown that Equation 3c considered the size effect, however, (Bazant & Cao, 1987) deemed that this equation exhibited no size effect, because it is based on plastic limit analysis and not on fracture mechanics, which is unjustified for specimens with short horizontal yielding plateau.

On the same manner, Eurocode 2 (EN1992-1-1, 2004) adopted Equation 4 to predict the punching shear stress, where the stress is act on distance 2d from the column face.

$$v_c = 0.18\sqrt[3]{f_{ck}} \times \left(1 + \sqrt{\frac{200}{d}}\right) \times \sqrt[3]{100\rho} \tag{4}$$

In Equation 4, the size effect is characterized by term $1 + \sqrt{\frac{200}{d}}$, in addition, the reinforcement ratio (ρ) is also considered. The salient aspect is that the concrete strength is introduced in terms of cubic root, (Marzouk & Hussein, 1992), found that the cubic root of the concrete strength is better to use in high strength concrete. Equations 3a, 3c, and Equation 4 were applied to current data results. The comparisons with experimental results are shown in Figure 6a. From this figure, it is clearly shown that these equations are underestimated and the safety factors reached 143% for specimen E1.25.

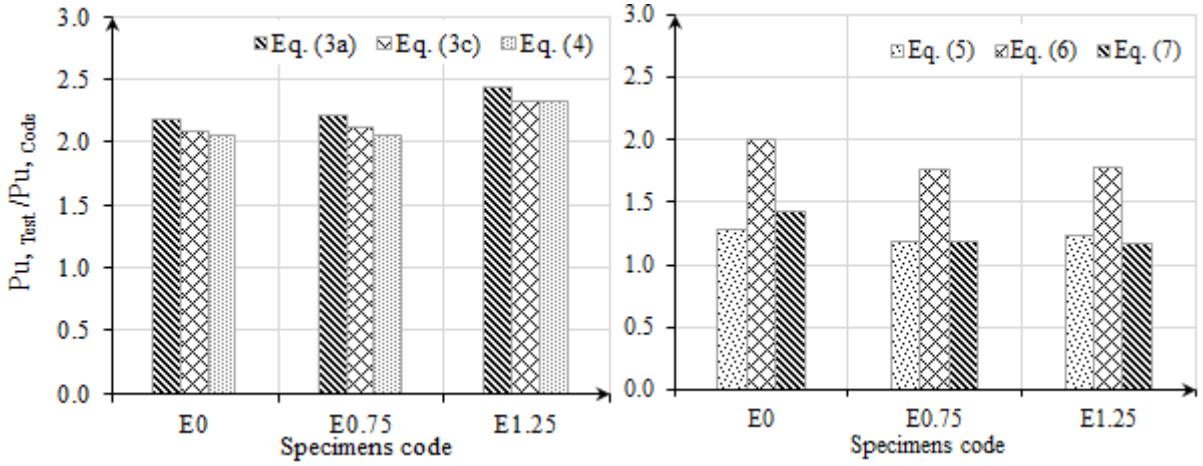

(a) (b)

Figure 6. Predicted punching shear resistance of current slabs according to (a) Equations 3a, 3c and 4 (b) Equation 5, 6, and 7

According to Proposed Models from Literature

For SFRC slabs, many Equations have been proposed to predict the punching shear stress based on Equation 3a, (Shaaban & Gesund, 1994; Harajli et al., 1995; De Hanai & Holanda, 2008), the three equations are listed respectively as below:

$$v_{SF} = \left(\frac{196.25 \times V_f}{w_c} + 0.567\right)\sqrt{f'_c} \quad (5)$$

$$v_{SF} = v_{c,ACI} + \left(0.096 \times V_f\right) \times \sqrt{f'_c} \quad (6)$$

$$v_{SF} = \left(0.15 \times V_f + 0.51\right)\sqrt{f'_c} \quad (7)$$

Applying aforementioned Equations (5-7) to the tested slabs and considering the stresses are acting on perimeter as proposed by ACI 318 (d/2 from the face of column) showed that the proposed equations are less conservatively than Equation 3a, because the steel fiber is taken into account (Figure 6b). Equations 5 and Equation 7 seem to give good prediction with safety factor 16% to 22% for specimen with steel fiber.

4.Conclusion

The following conclusions can be derived from this research:

- Inclusions 1.25 percentage of steel fiber by volume of concrete led to enhance the ultimate punching shear resistance by 17% compared with the associated plain concrete slabs, but it is less than its effect on low strength concrete slabs, moreover steel fiber is reducing the deformation induced from different load stages, and decreases the diameter of critical shear crack.
- For two steel fiber percentages, there were no effect shown on the inclination of the punching shear cracks.
- All the tested slabs showed punching failure, but the slabs showed small horizontal plateau before reaching the displacement that corresponding to ultimate load.
- The provision of punching shear resistance of the two codes used in comparison (ACI 318, and Eurocode 2) are highly conservative for specimen in high strength concrete,

while the proposed model by (Shaaban & Gesund, 1994; De Hanai & Holanda, 2008) are less conservatively.

References

Abadel, A., T. Almusallam, Y. Al-Salloum , & H. Abbas. 2014 Punching Shear Strength of Steel Fiber Reinforced High Strength Concrete. *Proc. of the Second Intl. Conf. on Advances In Civil*, Structural and Environmental Engineering- ACSEE. USA: Institute of Research Engineers and Doctors. 236-239.

ACI318-14 *Building Code Requirements for Structural Concrete*. 2014, American Concrete Institute.

Bazant, Zdenek P., & Zhiping Cao. 1987. Size Effect in Punching Shear Failure of Slabs. *ACI Structural Journal* (American Concrete Institute), Title no. 84-S6, 44-53.

Choi , K.K., M.M.R Taha , H.G. Park , & A.K. Maji. 2007. Punching shear strength of interior concrete slab–column connections reinforced with steel fibers. *Cement & Concrete Composites* **29**, 409-420.

De Hanai, J.B., & K.M.A. Holanda. 2008. Similarities Between Punching and Shear Strength of Steel Fiber Reinforced Concrete (SFRC) Slabs and Beams. *Structures and Materials Journal (IBRACON)* **1**(1), 1-16.

EN1992-1-1. 2004 *Eurocode 2: Design of concrete structures - Part 1-1: General rules and rules for buildings* 2004,. CEN, Brussels.

Gardner, N. J. 1990. Relationship of the Punching Shear Capacity of Reinforced Concrete Slabs with Concrete Strength. *ACI Structural Journal*. **87** (1), 66-71.

Gouveia , N.D., N.A.G. Fernandes , D.M.V. Faria, A.M.P. Ramos, & V.J.G. Lúcio. 2014 SFRC flat slabs punching behaviour – Experimental research. *Composites: Part B* **63**, 161-171.

Harajli, M.H., D. Maalouf , & H. Khatib. 1995. Effect of Fibers on the Punching Shear Strength of Slab-Column Connections. *Cement & Concrete Composites (Elsevier Science Ltd.)*. **7**, 161-170.

Marzouk , H., & A. Hussein. 1992. Experimental Investigation on the Behavior of High-Strength Concrete Slabs. *ACI Structural Journal (American Concrete Institute)*. **88** (6), 701-713.

Shaaban , A.M., &H. Gesund. 1994. Punching Shear Strength of Steel Fiber Reinforced Concrete Flat Plates. *ACI Structural Journal (American Concrete Institute)*. **91**(3), 406-414.

Shah, S. P. 1981. Fibre Reinforced Concrete. *Concrete Construction*. 26 (3), 261-266.

Swamy , R.N., & S.A.R. Ali. 1982. Punching Shear Behavior of Reinforced Slab-Column Connections Made with Steel Fiber Concrete. *ACI Journal (American Concrete Institute)*. Title no. 79-4, 1392-406.